2014 IEEE International Conference on Robotics & Automation (ICRA)
Hong Kong Convention and Exhibition Center
May 31 - June 7, 2014. Hong Kong, China

Heading alignment with summarized inertial pose constraints

Dehann Fourie, Kenny Uren, and George van Schoor

***Abstract*— A discontinuity seems to exist in present aided inertial navigation systems – the operational availability of high cost inertial navigation currently depends on the availability of a valid GPS lock. In general GPS solutions can be two or more orders cheaper than their inertial sensors counterparts. This paper addresses the north alignment by gyrocompassing in the context of more modern smoothing techniques. Incremental smoothing is becoming a serious contender for *in-situ* state estimation. The work here presents a probabilistic model for north alignment with an analysis towards the achievable accuracy of such a system. A *pose graph* formulation is used to estimate inertial sensor calibration terms over a long spanning trajectory, from which a true north alignment can be extracted. The *preintegral* method is used to condense high rate inertial data, but allow for post integration bias correction. Results show that the proposed alignment scheme is feasible, and would for gyrocompassing alignment relaxed sensor performance constraints.**

I. Introduction

Large robotic equipment and vehicles often require good state navigational state estimates. Various navigational aids are available for different situations. Inertial measurement units are often employed in combination with aiding sensors such as global positioning system (GPS) satellite navigation. Higher class inertial sensors are often required to obtain an unaided true north through measurement of the earths rotation rate. In 1984, Johnson presented a continuous adaptive gyrocompassing technique without external aiding measurements such as GPS [1]. Gyrocompassing, or inertial alignment, is considered a fundamental problem in navigation / localisation. Present approaches either assume prior knowledge of heading or build an inherent dependence on some absolute position or velocity measurement.

Higher class inertial gyroscopes are able to sense the earth's rotation rate and use it as an azimuthal alignment measurement for Inertial Navigation Systems (INS). Beyond high cost inertial solutions, magnetic and GPS techniques are generally used for lower cost absolute heading alignment. Alignment refers to process of estimating and obtaining confidence in the local level, north pointing direction.

Autonomous underwater vehicles (AUVs), by example, benefit a great deal from accurate heading alignment – by being able to navigate under water by dead reckoning. While a magnetic compass, acoustic navigational aids or even occasional surface GPS readings may be used to navigate a vehicle in open water; these navigation aids will be of little use when operating near ferrous materials, acoustic reflective surfaces or during submerged operation.

A. Overview

Section II presents a brief context at the state-of-the-art gyrocompassing. Contributions are presented, followed by a brief historical survey. The north alignment problem is defined in section III, and used as basis for deriving a probabilistic north alignment model. Methods and an analysis of achievable performance is presented near the end. A critical analysis of the proposed technique is given.

B. Contribution

An alternative formulation exists for the true north heading alignment problem. Heading alignment can be achieved during dynamic motion of the IMU cluster – extending the work of conventional carouselling schemes. This work differs in that the dynamic stimulus of the IMU is not a predefined carouselling scheme.

The motivation is based on an observation from the original mechanical gyrocompass. Mechanical systems are able to operate in dynamic environments – through Schuler tuning – without absolute position or velocity aiding measurements.

Present filtering based strapdown gyrocompass approaches mirror mechanical systems, by estimating only the current system state; permanently incorporating all errors and approximations into the state covariance matrix. This happens through the state marginalisation process inherent to recursive filtering. By example, the state residual update gain – sometimes the Kalman gain – becomes sub-optimal and bakes system errors into the single snapshot state estimate. Sigma Point Kalman filters, [2], improve on propagating state covariance through non-linear transforms, but still only considers a single snapshot in time.

Smoothing is gaining popularity and has the advantage of tractably maintaining long data streams; access to previous measurements are directly available to the optimisation process. This gives the user the privilege of hind sight, allowing one to go back and compute the *best fit* solutions to a collection of data. Intuitively then, one can expect a larger computational cost, but greater processing freedom than having to operate on single snapshots of estimated state.

Classical coarse alignment, section II-B, requires the system to remain stationary for a period of time and can take anything from a few minutes to hours. The stationary requirement exists because present unaided alignment formulations require undisrupted measurement of the small earth rotation rate signal. This paper shows an alternative method which exploits the advantages of smoothing. Modern smoothing allows computationally efficient methods to fuse information from various sensors and estimate observable system states.

978-1-4799-3684-7/14/$31.00 ©2014 IEEE

This paper illustrates that gyrocompassing can be done with *in-situ* smoothing. Alignment to an absolute North heading reference is achieved by firstly observing sensor error terms through non-absolute aiding measurements; after which the sensor errors are subtracted from the already measured data and then optimised towards the modeled earth rotation rate. More than that, measured earth rate and gravity can be used as the only absolute measurements made by the system. Aiding through use of only relative frame constraints can still be used to obtain a true north alignment in dynamic situations. The authors have not yet encountered a similar statement in public literature.

This statement may seem subtle, but implies absolute information is not required for an inertial based north alignment process. Relative constraints on position of velocity can be sufficient to aid an inertial solution towards a true north alignment. We do note, in this paper, we still assume absolute latitude is known as initial condition, however, filtering approaches have already shown one is able to estimate heading and platform latitude concurrently. These approaches still use high class sensors. From an operational standpoint, a user supplied latitude at start-up is not uncommon.

This paper shows that inertial sensors that were previously considered of too poor quality can be used to estimate a true north alignment. The operational premise is that many robotic systems operate over long time spans, and using the sensor data in a smoothing framework, allows the designer to extract true heading alignment from the dynamically calibrated inertial sensor measurements.

This paper presents the following contributions towards the state-of-the-art:

1) The concept of gyrocompassing with opportunistic modulation of the earth rotation rate signal;
2) A smoothing, rather than marginalising filter, data processing framework;
3) The use and preliminary impact analysis of using inertial preintegrals [3] for inertial constraints pose graph constraints [4]; and
4) Present the separation of concerns question – mixing of various performance sensors – in light of smoothing based approaches (Section VI-A).

Presently, little information, if any, has been found in the public domain relating to gyrocompassing in the manner presented here.

II. Brief Survey

A. History

The first mechanical gyrocompassing device was by Van den Bos in 1885, but he was unable to demonstrate a working prototype. Antshutz, in Germany, was able to demonstrate a working prototype around 1902. Iron-hull ships emerging, and saught after in the build up to the First World War. Ferrous materials, however, disrupted the magnetic compass. With the stimulus of war, and following a demonstration by Antshutz, Sperry developed his own gyrocompass and was widely used during WW I.

The gyrocompass consisted of a spinning mass, the axis of which would rotate relative to local level as the earth turned. Any misalignment of the gyro from the due East direction – zero earth rotation axis – produced would tend to deviate the system from a local vertical reference. Local vertical was obtained by measuring gravity. By servoing the spinning mass by about the vertical, with negative feedback, a useful North alignment could be obtained. A pendulum was an attractive option to establish the vertical, but was of little use under unknown platform accelerations.

Antshutz employed Max Schuler to resolve the "issue of the vertical" under unknown ship accelerations. His work, [5], resulted in an elegant and generic tuning method. Schuler noted that if the pendulum's centre of mass were to coincide with the centre of the earth, all lateral accelerations would not deflect the pendulum from the local vertical. That is a pendulum with harmonic oscillation at approximately $84.4\ min$.

In practice, a gyro-pendulum is used to emulate this oscillation period. This allowed the Antshutz system to successfully operate in dynamic marine environments. Today, Schuler tuning is widely employed as a Kalman Filtering tuning method for aided inertial navigation systems.

B. Direct Gyrocompassing

For linearized systems, an approximate heading angle must first be obtained at start-up. A process commonly referred to as coarse alignment. Direct trigonometry is used to extract heading alignment from horizontal gyroscope measurement components of earth rotation, ω_{ie}, [6], [7], [8], [9]:

$$\psi = \text{atan2}\ \frac{p}{q} \tag{1}$$

where, ψ is the local level north to body x axis angle. The triad of body measured rotation rates is $\omega^b = [p, q, r]^T$. Note, the forward-right-down convention is used respective to the body x-y-z axes.

This approach imposes two major requirements; Firstly, the system must remain stationary for some period to obtain the initial alignment. The coarse alignment period is dictated by the noise performance of the gyroscopes. Secondly, this direct approach imposes a severe requirement on the gyroscope bias [6].

C. Maytagging and Carouseling

Maytagging and continuous carouseling [10] methods have been employed to reduce the gyroscope bias performance requirements, or further increase the long term navigational accuracies of ship borne inertial navigation systems (SINS).

Johnson's work [1] is an carouseling extension of a stapdown gyrocomassing approach presented by Britting [6]. His study showed a two gyroscope system using a Kalman filter for heading alignment, supplemented with a secondary low pass filter and accelerometers to resolve the local vertical. More recently, Renkoski [11] investigated multidimensional, but periodic carouseling patterns.

The advantage being, carouseling modulates the earth rate signal allowing the designer to discern the earth rate from the sensor biases. In some way, the next step is to incorporate an *opportunistic* modulation scheme, rather than strictly periodic to the gyrocompassing process. The intention furthermore is to use the motion of the platform as the random modulation signal. The premise then is that smoothing, over filtering, is better suited towards such a goal.

D. Optical Landmark Alignment

Optical heading alignment – widely used by surveyors – relies on sighting of landmarks at known locations. Planar geometry allows one to resolve the objective north alignment from several sightings. Electronic versions of such systems are known to exist and are mostly used in the maritime setting, whereby a ship's compass can be aligned more quickly through sightings of known landmarks.

E. Absolute Position and Velocity Aiding

Probably the most dominant approach used in aided inertial navigation today, is where inertial position and velocity solutions are aided by absolute external references such as GPS [9], [12]. Furthermore, aiding of the inertial solution is generally done with an extended Kalman filter (EKF).

The standard mechanisation derives an orientation estimate from the gyroscope measurements and projects body measured accelerations into the estimated navigational frame. The projected accelerations can, in turn, be double integrated to obtain velocity and position estimates. While estimation errors in pitch and roll are observable through the gravity vector [8], the heading angle is generally extracted through residual lateral velocities. Mismatches between inertially predicted lateral motion the aiding velocity measurement is fed back to better align the platform course.

F. Filtering

The EKF is the workhorse of most modern aided inertial navigation systems [8]. The Jacobian derivative method used by the EKF is sensitive to initialisation errors [12], enforcing the *coarse* heading alignment requirements. The EKF filters have an even larger drawback, in that they marginalise errors from previous states, permanently *baking* errors into the single snapshot estimate. Errors in state and covariance estimates are artificially bled from the solution using process noise, without recourse.

This *baking* problem is of particular concern to uninitialised non-linear attitude dynamics. These errors are commonly dealt with through tighter linearisation requirements, increasing process noise or the use of iterative filtering methods [13]. Process noise effectively allows outside measurement information to influence the state estimates more than the internal models predict and presents a rather crude approach, overpowering the delicate gyrocompassing task.

In 2006 Ahn, [14], showed how different strapdown attitude filter parameterisations influence the gyrocompassing performance. Use of an angle axis misalignment parameterisation in the filter improved observability of the gyrocompassing process. Maintaining proper manifold mechanisations will avoid mapping and projection related problems. This aspect is one of the main contributions of the large heading uncertainty EKF models presented by Kong [15].

III. Problem Statement

The main problem to address is how to align a robotic system to the local north reference, starting with no prior information, without absolute aiding information, on a moving platform.

IV. Theory

Fig. 1 presents a conceptual time snapshot view of true and predicted north heading. It is desirable to have the platform which is free to rotate, while refining its north alignment as more measurements are gathered. The instantaneous direction of the measurement body is denoted by x, and heading misalignment is denoted by A.

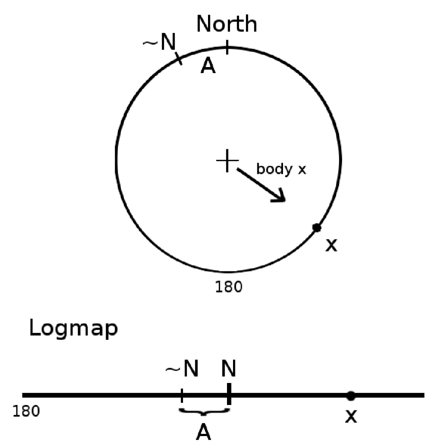

Fig. 1. A conceptual view of true and estimated north at any point in time. The projections are shown on the manifold with the platform forward axis direction, x, decoupled from the alignment process and is free to rotate.

Angular manifolds are used to describe rotational transforms. Taylor [16] mentions how several manifolds exist for batch optimisation methods. The most commonly used in the conventional inertial navigation is the incremental tangent space. This is equivalent to the linear small angle assumption that is commonly used in the derivation of the EKF based architectures.

Algorithms which process strapdown inertial sensor information must be able to handle sensor errors. It has become common place to dynamically estimate sensor bias terms with a Kalman filter through aiding information. The filter uses process and measurement noise as terms to allow for *softness* in the estimation process. It is imperative then, that we introduce similar flexibility regarding sensor measurements in the smoothing context.

Some challenges surrounding the orientations for pose graph optimisation were highlighted in a recent paper by Carlone [17]. Carlone's paper mentions the difficulty in estimating the maximum likelihood estimate of pose states due to orientation states at each node, which is effectively the consecutive compositionof trajectories on a rotational manifold. The orientation states have a non-trivial topology, making the problem highly non-linear and non-convex. Carlone's paper provides a multi-hypotheses global optimisation that does not suffer from local minima.

A. Alignment Process Definition

Consider the inertial heading alignment process within a *factor graph* framework. A generalised representation of system state variables, whereby relations between the variables are defined in a manner which impose fewer assumptions than current filtering methods. This freedom allows greater flexibility in the capabilities of the final system. The factor graph encodes the constraints between variables, which are then optimised through various non-linear optimisation techniques (see section IV-D).

Pose graphs are a special case of factor graphs where the navigational states of the system are represented by poses at discrete time instances, shown as the green nodes in fig. 2. Furthermore, Bell [13] showed the equivalence between iterated filtering, used as smoother, and direct non-linear optimisation of structures which are now referred to as *factor graphs*.

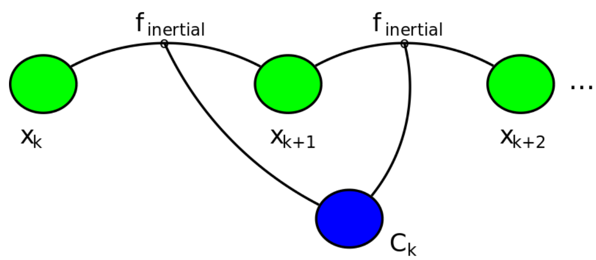

Fig. 2. Trivial *factor graph* showing pose variable states as green nodes, for time instances t_k, t_{k+1} and t_{k+2}, and inertial residual constraints $\mathbf{f}_{inertial}$. The inertial residual constraints depend on sensor error and alignment variable in the blue node C_k.

Constraints between the pose states are established by allocating a cost function to the residual error between predicted and measured values. Measurements gathered from the inertial measurement unit (IMU) are used to define factor nodes between successive variable nodes. The expected gravity and earth rotation rate parameters are then captured in the factor node cost functions. Notice that the factor graph, other than the initial condition, is not anchored to absolute reference information other than inherently measured earth rotation and gravity.

Alignment is achieved through optimisation of the measurement residuals captured in the inertial constraints, given later in (14). North alignment becomes possible by separating gyro sensor biases from the earth rotation rate, in the same way that pitch and roll alignment with the local level is done by separating accelerometer biases from measured gravity. This is made possible under the assumption of modulation of the earth rate and gravity signals.

Indelman [4] showed it is not practical to incorporate high rate inertial measurements directly in a factor graph formulation. Around the same time, Lupton, [3] proposed the use of inertial *preintegrals*, and was later adopted by Indelman in [4] as direct inertial pose graph constraints.

B. Probabilistic Model for North Alignment

The starting point for the mathematical manipulations presented below are based on two fundamental ideas:

1) We can represent the north alignment as a probability function, which depends on measurements from a sufficient set of sensors; and
2) We can factorise the probability function as the product of individual functions based on separate, independent, measurements from the sensors. A sparse data representation can be constructed, and can then be solved through a non-linear optimisation process.

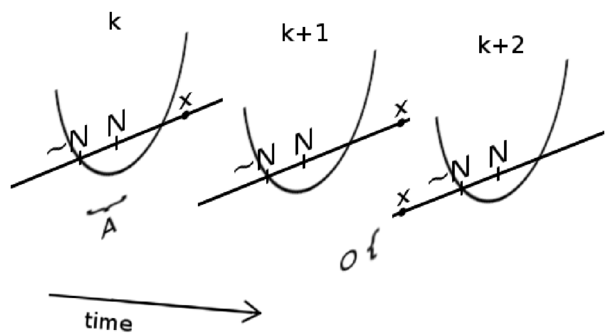

Fig. 3. Conceptual view of multiple poses being optimised. Heading misalignment is shown as 'A' on the straight lines representing the logarithmic map of the yaw angle on a manifold. The Gaussian cost of heading prediction measurement residual is depicted by the parabola. The remaining cost of misalignment in the system is shown as 'O'. True north is shown through 'N' and the current estimated north is shown as 'Ñ'. Variable 'x' represents the current body X axis direction.

Portions of the notation from [18] are used here. Consider a set state variables, up to time t_k, are to be estimated, and are collected in a set $\mathcal{V}_k$:

$$\mathcal{V}_k \doteq \{X_k, C_k\} \tag{2}$$

where X_k are the normal state variables and C_k are sensor calibration state variables. The joint probability distribution of all the variables can be abstracted as:

$$p\left(\mathcal{V}_k | \mathcal{Z}_k\right) \tag{3}$$

That is the probability distribution of the function for all the system variables, given the collection of measurements which have been made until that point in time $\mathcal{Z}_k$. The best fit solution to all the measurements can then be found by inferring the maximum a posteriori (MAP) estimate of all variables which have been included in the system up to that point in time. This can be written as:

$$\mathcal{V}_k^* = \underset{\mathcal{V}_k}{\operatorname{argmax}}\, p\left(\mathcal{V}_k | \mathcal{Z}_k\right) \tag{4}$$

where, $\mathcal{V}_k^*$ represents the optimal assignment of estimated variables to the available measurement information. This *optimal* assignment of values to state variables is subject to the assumptions made during the optimisation process. The choice of probability distribution and inference method are main factors.

With this in hand, the north alignment problem can be written as an optimisation problem. The focus now shifts to how inference is drawn on the joint probability distribution in the context of inertial measurements. The problem is broken down by using a factor graph representation of the state variable and measurement information.

1) Graphical Model Representation: Factor graphs [19] have become a popular representation in the simultaneous localisation and mapping (SLAM) community. *Factor graphs* consist of *factor*, representing some constraint, and *variable nodes* representing the variables being estimated by the system. The *nodes* encode the relation between state variables which are to be estimated. *Factor graphs* effectively encode the factorisation of the global joint probability function, given in (3), in that each factor node represents an individual term of the global joint probability:

$$p\left(\mathcal{V}_k|\mathcal{Z}_k\right) \propto \prod_i f_i\left(\mathcal{V}_k^i, \mathcal{Z}_k\right) \tag{5}$$

where, $\mathcal{V}_k^i$ is the subset of variables involved with individual constraint function f_i. The optimisation problem presented by (4) and (5) can be solved by letting each factor node represent a costing operation $\mathcal{D}\{\}$.

$$f_i\left(\mathcal{V}_k^i, \mathcal{Z}_k^i\right) = \mathcal{D}\{\delta_k^i\} \tag{6}$$

with, δ_k^i representing the prediction-measurement residual:

$$\delta_k^i = h_i\left(\mathcal{V}_k^i\right) - \mathcal{Z}_k^i \tag{7}$$

If the residual cost function is assumed to be Gaussian, the optimisation simplifies to the least squares best fit solution. The cost function is represented by the normal distribution function:

$$\mathcal{D}\left\{\delta_k^i\right\} = exp\left(-\frac{1}{2}\ {\delta_k^i}^T {\Lambda_i}^{-1} \delta_k^i\right) \tag{8}$$

where, ^{T} denotes the transpose, and Λ_i is a weighting covariance matrix, effectively the Mahalanobis distance squared. Note that selection of the cost function is not restricted to only the Gaussian case. Other cost functions have been used in analogous iterated optimisation structures, including the pseudo-Huber or t-distribution [20]. While different cost functions may promote certain desirable properties – including robustness or better error distribution modelling – it is not the focus of this paper.

The Gaussian residual assumption simplifies the optimisation in that the proportional constraint in (6), and following from (4), we can manipulate the system objective expression; keep in mind that multiplying the costing function by a constant value does not vary the location of the optimum point:

$$\mathcal{V}_k^* = \underset{\mathcal{V}_k}{\operatorname{argmin}} \left[-\log f\left(\mathcal{V}_k, \mathcal{Z}_k\right)\right] \tag{9}$$

$$= \underset{\mathcal{V}_k}{\operatorname{argmin}} \left[-\log\ exp\left(-\frac{1}{2}\ {\delta_k}^T \Lambda^{-1} \delta_k\right)\right] \tag{10}$$

Note, in the above equation we have stacked individual prediction and measurement data into a single residual vector δ_k. Next, we simplify the logarithm exponent pair and drop the half in the exponent:

$$\mathcal{V}_k^* = \underset{\mathcal{V}_k}{\operatorname{argmin}} \left\|\mathbf{h}\left(\mathcal{V}_k\right) - \mathcal{Z}_k\right\|_\Lambda^2 \tag{11}$$

where, following from (8), we use the shorthand $\|\delta_k\|_\Lambda^2 = {\delta_k}^T \Lambda^{-1} \delta_k$.

C. Inertial Factors

The gyrocompassing task relies on the solution of (11), given inertial constraint factors which are sensitive to heading alignment and gyroscope bias. Given sufficient data, the heading and biases become observable and can be estimated by the optimisation process. The minimum cost assignment of variable $\mathcal{V}_k$ therefore represents the best estimate of heading alignment and sensor bias, for data until time k.

As a consequence, inertial factor constraints must be formulated such that bias and heading alignment errors can be subtracted from the constraint terms. In the conventional inertial sensor integration sense this is a difficult operation. A further problem, as was encountered in [4], is that inertial measurements are usually taken at a high rate and would result in a large system of equations. The inertial *preintegral* method proposed by Lupton [3] introduces a way to circumvent both these problems.

At this point we should remember that some early gyroscopes are referred to as rate integrating designs, whereby forces or rates are mechanically integrated and measurements are presented as an accumulated value for the sample period. Many modern strapdown sensors still support delta angle and delta velocity modes.

1) Inertial preintegrals: Present state-of-the-art techniques build upon integration of high rate samples, after bias and gravity corrections have been applied. However, under the MAP computation framework errors in the bias and gravity components must be tractable: Stated differently, iterative refinement of estimates update the state estimate. As a consequence the linearisation point used for the constraint functions also change. The manner in which inertial data are used in the graphical model must therefore allow the user to update and modify these already integrated perturbations.

Inertial *preintegrals* offer a convenient manner to summarise inertial measurements, but allow a mechanism whereby the mentioned errors can be updated in a tractable manner. To reduce the amount of inertial constraints, the measurements are integrated over any time period as a summary of motion. Summarising high rate data reduces the state size of the problem, but creates a trade-off in preintegral correction accuracy. The question becomes for how long should inertial data be summarised before it is added as constraint to the *pose graph*.

2) Summarising Inertial Measurements: The computations for *preintegrals* are split into two categories. The first is the summarising process whereby high rate inertial information is summarised, and the second on how errors within the *preintegrals* are compensated and used to perform inference within the probabilistic model.

The preintegrals are used to predict the platform heading by accumulating delta headings from each interpose constraint. Interpose constraints formed by integrating IMU data relative to the previous pose:

$$\hat{R}_{b_{t_1}}^{b_{t_2}} = \prod_{t=t_1}^{t_2} expmap\left(\omega_t^b \Delta t\right) \tag{12}$$

where, $\Delta t = t_2 - t_1$ is the summary of motion from the high rate sensor information from time t_1 to t_2, and $\hat{R}_{b_{t_1}}^{b_{t_2}}$ is a rotation matrix representing the orientation between the two instances in time. The expansion here uses zeroth-order integration. Savage [21] presents more accurate methods, including the Picard solution, which further support coning, sculling and scrolling corrections in an efficient manner.

The heading angle, relative to the present estimate local navigational frame, is predicted with the current interpose delta in addition to the previous pose estimated navigational orientation:

$$\hat{R}_{b_{k+1}}^{n} = \hat{R}_{b_k}^{n} \hat{R}_{b_{t_k}}^{b_{t_k+\Delta t}} \tag{13}$$

Since we do not know the initial heading, we assume it to be zero. The optimisation process will be able to observe the global heading alignment of the system once sufficient information has been gathered to overcome sensor noise limitations.

Gyroscope sensor noise is an important consideration for gyrocompassing systems. Noise creates uncertainty in the measurement and is only reduced at a rate of the square root of sample number. In the conventional sense of strapdown *coarse aliment*, a doubling of sensor noise would induce a square on the time required to measure the earth's rotation rate to the same accuracy.

3) Inertial Inference: The second step is the probabilistic inference step whereby predicted navigational states are inferred from the *preintegrals* and effectively allows the user to extract use pose updates and correct compensation terms. The predicted mean is computed by:

$$h\left(x, C\right) = \left(w_{ie}^{L}\ cos(\psi + \delta\psi + \delta\omega_{\psi}\Delta t) + \delta\omega_v\right)\Delta t \tag{14}$$

where, $x = [\psi]$ is the pose predicted heading variable. The calibration states are denoted by $C = [\delta\psi, \delta\omega_\psi, \delta\omega_v]^T$, representing heading misalignment, yaw gyro bias and vertical gyro bias errors. Local horizontal north pointing earth rotation rate is given by $\omega_{ie}^{L} = \cos\lambda$, where λ is the latitude.

The measurement prediction residual is computed with:

$$\delta_k = h\left(x, C\right)|_{t_1} - \mathcal{Z}_k^{heading} \tag{15}$$

$$\mathcal{Z}_k = logmap\left(\hat{R}_{b_{k+1}}^{n}\right) \tag{16}$$

D. Optimisation Solutions

Eq. (11) is the link between a *pose graph* representation of the north alignment problem and numerical optimisation techniques. A great many techniques – including Newton, gradient descent and trust-region – exist for optimising problems of this form. Furthermore, the work of Kaess et al. [22] allow incremental solution of such problems. This paper is not focussed on the method used to solve (11), however a few considerations must be highlighted.

The system encoded by the *pose graph* must be observable: There should be more constraint than degrees of freedom in the system. Eq. (11) effectively describes a nonlinear regression problem. In general, the north alignment problem will be over-defined and variables can be estimated with greater accuracy as more measurement data is included in the regression process– analogous to solutions of the *SLAM* problem in robotics.

V. Results

In this section we present results through simulation of the theory presented in the previous sections. Simulation intends to determine the accuracy and feasibility of north alignment under variation of some model parameters. The main outcome of this exercise is to determine how much of an influence gyroscope noise, and *preintegral* summary period have on the gyrocompassing outcome. A further aspect is whether there is a significant improvement between higher or lower bandwidth random modulation of the earth rate signal.

Solution of the optimisation problem presented in (11) is done with MATLABs optimisation toolbox.

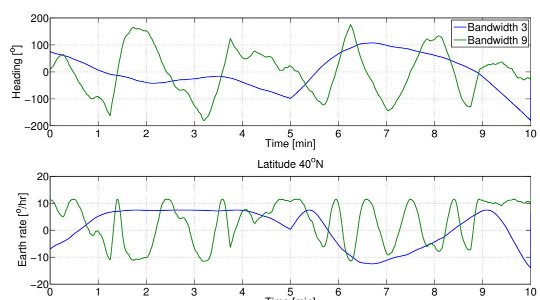

Fig. 4. Two randomised sample heading trajectories to illustrate difference between a higher and lower bandwidth models. Bottom figure shows respective modulated earth rate signals for a system assumed to be at 40^o latitude.

The simulated system is concerned with extracting north alignment from strapdown sensors which are rotated about the vertical axis during the north alignment process. It is assumed that a vertical reference is available through accelerometer based measurement of the the gravity vector. Assuming then that pitch and roll angles are available to some accuracy, we are only concerned with the horizontal components of the measured earth rotation rate.

Furthermore, the measurements are made from a dynamical platform reducing the requirement for dual orthogonal rate measurement. Clearly a full 6DOF mechanisation will be required to use this system in practice, but [18] has already shown that this is possible. This paper is concerned with whether a smoothing mechanisation can be used effectively for gyrocompassing. Furthermore, Schuler tuning has already shown that gyrocompassing is possible in the presence of disturbance accelerations.

The simulation mechanises a single horizontal measuring gyroscope and a vertical measuring yaw angle gyroscope. The system is randomly rotated about the vertical axis for a spread of higher and lower bandwidth trajectories. Two example trajectories are shown in fig. 4. The bandwidth parameter is defined as a heuristic parameter between 0 and 10, representing a range of motion from nearly stationary to high rotational dynamics. Gyroscope measurements data rate is set at 100 samples per second.

Section IV-C.2 presented inertial *preintegrals*. The *preintegrals* are formed by summarising high rate inertial data for a period Δt. Compensation terms for errors in the preintegrals are subtracted from the *preintegrals* during the inertial inference step. The compensation terms represent integrals of the error components in the *preintegrals*, but integrated by a single large zeroth-order integration step. Large integration errors here will disrupt the achievable alignment accuracy of the system.

Fig. 5 shows the achievable RMS heading alignment from a randomised heading and gyroscope bias. Figures were obtained by drawing the root mean square performance for 500 runs per data point. The figure is computed for a gyroscope measurement noise parameter, set at $\sigma = 3\ ^0/hr$.

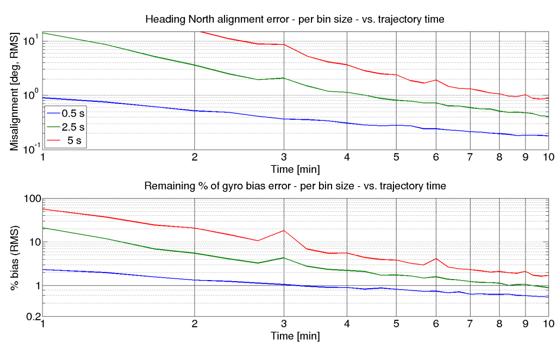

Fig. 5. Top figure shows RMS alignment accuracy over time in minutes, across three inertial *preintegral* bin sizes. The lower figure shows the bias estimation accuracy as a percentage of gyro bias remaining after the inertial inference correction process.

While fig. 5 presents RMS performance over gyrocompassing time, there is an interesting relation between the gyro measurement noise and *preintegral* bin time variation. Fig. 6 shows misalignment and gyro bias estimation accuracy for a fixed gyrocompassing time of $10\ mins$, but with a variation of gyroscope measurement noise performance. Similar bin size variations are maintained.

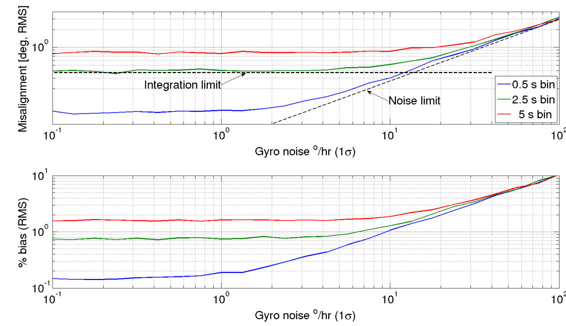

Fig. 6. Figure showing two gyrocompassing RMS performance boundaries. The top figure shows remaining misalignment error after $10\ mins$ of gyrocompassing. Three *preintegral* bin sizes are shown as individual curves. Gyroscope measurement noise and *preintegral* integration errors are indicated. The lower figures shows the

Based on curve gradients, two asymptotic system error sources can be seen in fig. 6. The first is associated with gyroscope measurement noise, indicated as *noise limit*, and places a lower bound on the achievable gyrocompassing accuracy. The second is the level gradient, denoted *integration limit*, associated with the zeroth-order integration term in (14). This too presents a lower bound on alignment performance, and is a function of the *preintegral* bin size.

A last result, shown in fig. 7, indicates the sensitivity to variation in sensor noise. Here the bin size is fixed and performance is determined based on the available gyrocompassing time. As more gyrocompassing data is collected, a more accurate the solution can be estimated. The results here show that heading alignment through gyrocompassing principles is possible in the probabilistic framework. The next section gives a critical analysis.

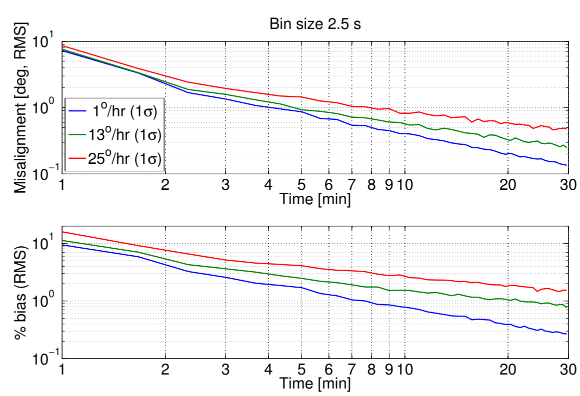

Fig. 7. The top figure shows RMS misalignment estimation accuracy over time, for three gyroscope measurement noise performances. The bottom figure shows the associated bias estimation accuracy.

VI. Critical Analysis

Fibre Optic Gyroscopes (FOG) and modern MicroElectro-Mechanical Systems (MEMS) gyroscopes are becoming a dominant technology in the inertial sensor market, replacing older and more expensive Ring Laser (RLG) and mechanical Dynamically Tuned (DTG) technologies. Inertial sensor cost is driven by four main desired performance factors: These include measurement noise, bias, volumetric size and power consumption. While further improvements in these areas remain difficult, newer data processing techniques can support the north alignment requirement.

The process presented in this paper shows that north alignment can be done with a relaxation of some sensor performance and operational requirements. The method extends the idea of existing carouselled systems, and proposes a replacement for filter based aided navigation approaches. Smoothing gives the designer the ability to maintain and reuse all measured data which has been gathered, and in turn allows simultaneous refinement of gyroscope bias and system misalignment estimates.

A. Separation of Concerns

An additional and recurring question within the inertial navigation community is whether sensors of different performance can be mixed in a single IMU cluster. Cost or volumetric constraints are general reasons for wanting to do this. Consider a terrestrial robot which on average does not pitch or roll significantly. One could argue that gyroscope accuracy requirements for these axes could be relaxed, while maintaining a better quality gyroscope for the heading estimate.

Mixing of sensor qualities to save costs does make intuitive sense, but unfortunately does not hold. Many groups have tried this, and the general response is that through dynamics the heading estimate is degraded through marginalisation and projection of measurements from the lower quality sensors onto the "accuracy sensitive" axis.

By adding a low dynamics assumption to some subset of estimate parameters, smoothing may present the further advantage – being able to track how much good or bad sensor information is being projected onto the respective reference frame axes across the entire trajectory. A projection from a poorer sensor only affects a limited number of poses in the sapce of the entire trajectory. Although estimate propagation is still based on this degraded measurement, marginalisation does not occur and thereby avoids the *baking* problem. The event is temporally contained to in time and space, allowing greater separation of concerns during estimation process.

VII. Conclusion

Many robotic applications rely on accurate heading alignment. Presently, most systems meet this requirement by adding a low-cost GPS or magnetometer dependency. Other applications, including underwater robotics, may not have access to either such measurements. Methods such as acoustic ranging or terrain referenced navigation exist, but are difficult in cluttered, dynamic or ferrous environments. Gyrocompassing is the only self contained alternative for heading alignment, and given recent developments in smoothing, it is important to reconsider the strapdown gyrocompassing process in that regard. Smoothing offers many advantages over the limitations inherent to the current dominant EKF method.

the computation of an efficient incremental update to $\bar{g}$.

References

[1] C. Johnson, "Adaptive corrective alignment for a carouseling strapdown ins," in *American Control Conference, 1984*, pp. 1856–1861, IEEE, 1984.

[2] S. J. Julier and J. K. Uhlmann, "Unscented filtering and nonlinear estimation," *Proceedings of the IEEE*, vol. 92, no. 3, pp. 401–422, 2004.

[3] T. Lupton and S. Sukkarieh, "Visual-inertial-aided navigation for high-dynamic motion in built environments without initial conditions," *Robotics, IEEE Transactions on*, vol. 28, no. 1, pp. 61–76, 2012.

[4] V. Indelman, S. Williams, M. Kaess, and F. Dellaert, "Factor graph based incremental smoothing in inertial navigation systems," in *Information Fusion (FUSION), 2012 15th International Conference on*, pp. 2154–2161, IEEE, 2012.

[5] W. Wrigley, "Schuler tuning characteristics in navigational instruments," *Navigation*, vol. 2, no. 8, pp. 282–290, 1950.

[6] K. R. Britting, *Inertial Navigation Systems Analysis*. 1971.

[7] A. Chatfield, *Fundamentals of High Accuracy Inertial Navigation*, vol. 174. AIAA, 1997.

[8] P. D. Groves, *Principles of GNSS, inertial, and multisensor integrated navigation systems*. Artech House, GNSS Technology and Application Series, 2008.

[9] D. Titterton and J. Weston, *Strapdown inertial navigation technology*, vol. 17. IET, 2004.

[10] M. S. Grewal, L. R. Weill, and A. P. Andrews, *Global positioning systems, inertial navigation, and integration*. John Wiley & Sons, 2007.

[11] B. M. Renkoski, "The effect of carouseling on MEMS IMU performance for gyrocompassing applications," Master's thesis, Massachusetts Institute of Technology, 2008.

[12] J. Farrell, *Aided navigation: GPS with high rate sensors*. McGraw-Hill New York, 2008.

[13] B. M. Bell, "The iterated kalman smoother as a gauss-newton method," *SIAM Journal on Optimization*, vol. 4, no. 3, pp. 626–636, 1994.

[14] H.-S. Ahn and C.-H. Won, "Fast alignment using rotation vector and adaptive kalman filter," *Aerospace and Electronic Systems, IEEE Transactions on*, vol. 42, no. 1, pp. 70–83, 2006.

[15] X. Kong, *Inertial navigation system algorithms for low cost IMU*. PhD thesis, Department of Mechanical and Mechatronic Engineering, Graduate School of Engineering, University of Sydney, 2000.

[16] C. J. Taylor and D. J. Kriegman, "Minimization on the lie group so (3) and related manifolds," tech. rep., Yale University, 1994.

[17] L. Carlone and A. Censi, "From angular manifolds to the integer lattice: Guaranteed orientation estimation with application to pose graph optimization," *arXiv preprint arXiv:1211.3063*, 2012.

[18] V. Indelman, S. Williams, M. Kaess, and F. Dellaert, "Information fusion in navigation systems via factor graph based incremental smoothing," *Robotics and Autonomous Systems*, 2013.

[19] F. Kschischang, B. Frey, and H.-A. Loeliger, "Factor graphs and the sum-product algorithm," *IEEE Trans. Inf. Theory*, vol. 47, Feb. 2001.

[20] C. Kerl, J. Sturm, and D. Cremers, "Robust odometry estimation for rgb-d cameras," ICRA, 2013.

[21] P. G. Savage, "A unified mathematical framework for strapdown algorithm design," *Journal of Guidance, Control, and Dynamics*, vol. 29, no. 2, pp. 237–249, 2006.

[22] M. Kaess, H. Johannsson, R. Roberts, V. Ila, J. Leonard, and F. Dellaert, "iSAM2: Incremental smoothing and mapping with fluid relinearization and incremental variable reordering," in *IEEE Intl. Conf. on Robotics and Automation (ICRA)*, (Shanghai, China), May 2011.